REPORT DOCUMENTATION PAGE

Form Approved OMB NO. 0704-0188

1. REPORT DATE (DD-MM-YYYY)	2. REPORT TYPE	3. DATES COVERED (From - To)
11-02-2016	Final Report	16-Feb-2012 - 15-Oct-2015

4. TITLE AND SUBTITLE
Final Report: A New Computational Tool For Understanding Light-Matter Interactions

5a. CONTRACT NUMBER
W911NF-12-1-0072

5b. GRANT NUMBER

5c. PROGRAM ELEMENT NUMBER
206022

6. AUTHORS
Gang Lu

5d. PROJECT NUMBER

5e. TASK NUMBER

5f. WORK UNIT NUMBER

7. PERFORMING ORGANIZATION NAMES AND ADDRESSES
California State University - Northridge
18111 Nordhoff Street

Northridge, CA 91330 -8232

8. PERFORMING ORGANIZATION REPORT NUMBER

9. SPONSORING/MONITORING AGENCY NAME(S) AND ADDRESS (ES)
U.S. Army Research Office
P.O. Box 12211
Research Triangle Park, NC 27709-2211

10. SPONSOR/MONITOR'S ACRONYM(S)
ARO

11. SPONSOR/MONITOR'S REPORT NUMBER(S)
60525-EL-REP.3

12. DISTRIBUTION AVAILIBILITY STATEMENT
Approved for Public Release; Distribution Unlimited

13. SUPPLEMENTARY NOTES
The views, opinions and/or findings contained in this report are those of the author(s) and should not contrued as an official Department of the Army position, policy or decision, unless so designated by other documentation.

14. ABSTRACT
Plasmonic resonance of a metallic nanostructure results from coherent motion of its conduction electrons driven by incident light. At the resonance, the induced dipole in the nanostructure is proportional to the number of the conduction electrons, hence 10-million times larger than that in an atom. The interaction energy between the induced dipole and fluctuating virtual field of the incident light can reach a few tenths of an eV. Therefore, the classical electromagnetism dominating the field may become inadequate. We propose that quantum electrodynamics (QED) may be used as a fundamental theory to describe the interaction between the virtual field

15. SUBJECT TERMS
Plasmonics, light-matter interaction, time-dependent density functional theory, modeling and simulations

16. SECURITY CLASSIFICATION OF:			17. LIMITATION OF ABSTRACT	15. NUMBER OF PAGES	19a. NAME OF RESPONSIBLE PERSON
a. REPORT	b. ABSTRACT	c. THIS PAGE			Gang Lu
UU	UU	UU	UU		19b. TELEPHONE NUMBER 818-677-2021

Report Title

Final Report: A New Computational Tool For Understanding Light-Matter Interactions

ABSTRACT

Plasmonic resonance of a metallic nanostructure results from coherent motion of its conduction electrons driven by incident light. At the resonance, the induced dipole in the nanostructure is proportional to the number of the conduction electrons, hence 10-million times larger than that in an atom. The interaction energy between the induced dipole and fluctuating virtual field of the incident light can reach a few tenths of an eV. Therefore, the classical electromagnetism dominating the field may become inadequate. We propose that quantum electrodynamics (QED) may be used as a fundamental theory to describe the interaction between the virtual field and the oscillating electrons. Based on QED, we derive analytic expressions for the plasmon resonant frequency, which depends on three easily accessible material parameters. The analytic theory reproduces very well the experimental data, and can be used in rational design of materials for plasmonic applications.

Enter List of papers submitted or published that acknowledge ARO support from the start of the project to the date of this printing. List the papers, including journal references, in the following categories:

(a) Papers published in peer-reviewed journals (N/A for none)

Received	Paper
08/25/2014 2.00	Hongping Xiang, Xu Zhang, Daniel Neuhauser, Gang Lu. Size-Dependent Plasmonic Resonances from Large-Scale Quantum Simulations, The Journal of Physical Chemistry Letters, (04 2014): 0. doi: 10.1021/jz500216t
TOTAL:	**1**

Number of Papers published in peer-reviewed journals:

(b) Papers published in non-peer-reviewed journals (N/A for none)

Received	Paper
TOTAL:	

Number of Papers published in non peer-reviewed journals:

(c) Presentations

Number of Presentations: 1.00

Non Peer-Reviewed Conference Proceeding publications (other than abstracts):

Received Paper

TOTAL:

Number of Non Peer-Reviewed Conference Proceeding publications (other than abstracts):

Peer-Reviewed Conference Proceeding publications (other than abstracts):

Received Paper

TOTAL:

Number of Peer-Reviewed Conference Proceeding publications (other than abstracts):

(d) Manuscripts

Received Paper

TOTAL:

Number of Manuscripts:

Books

Received Book

TOTAL:

Received Book Chapter

TOTAL:

Patents Submitted

Patents Awarded

Awards

Graduate Students

NAME	PERCENT_SUPPORTED	Discipline
Jeremy Del Aguila	1.00	
FTE Equivalent:	**1.00**	
Total Number:	**1**	

Names of Post Doctorates

NAME	PERCENT_SUPPORTED
Mingliang Zhang	1.00
FTE Equivalent:	**1.00**
Total Number:	**1**

Names of Faculty Supported

NAME	PERCENT_SUPPORTED	National Academy Member
Gang Lu	1.00	
FTE Equivalent:	**1.00**	
Total Number:	**1**	

Names of Under Graduate students supported

NAME	PERCENT_SUPPORTED
FTE Equivalent:	
Total Number:	

Student Metrics

This section only applies to graduating undergraduates supported by this agreement in this reporting period

The number of undergraduates funded by this agreement who graduated during this period: 0.00

The number of undergraduates funded by this agreement who graduated during this period with a degree in science, mathematics, engineering, or technology fields:..... 0.00

The number of undergraduates funded by your agreement who graduated during this period and will continue to pursue a graduate or Ph.D. degree in science, mathematics, engineering, or technology fields:..... 0.00

Number of graduating undergraduates who achieved a 3.5 GPA to 4.0 (4.0 max scale):..... 0.00

Number of graduating undergraduates funded by a DoD funded Center of Excellence grant for Education, Research and Engineering:..... 0.00

The number of undergraduates funded by your agreement who graduated during this period and intend to work for the Department of Defense 0.00

The number of undergraduates funded by your agreement who graduated during this period and will receive scholarships or fellowships for further studies in science, mathematics, engineering or technology fields: 0.00

Names of Personnel receiving masters degrees

NAME
Total Number:

Names of personnel receiving PHDs

NAME
Total Number:

Names of other research staff

NAME	PERCENT_SUPPORTED
FTE Equivalent:	
Total Number:	

Sub Contractors (DD882)

Inventions (DD882)

Scientific Progress

See Attachment.

Technology Transfer

A New Computational Tool For Understanding Light-Matter Interactions

Overview of the Project

In this project, the PI proposes to develop a new computational tool for understanding light-matter interactions in complex systems across multiple length and time scales from quantum dynamics to continuum electrodynamics. The new computational tool overcomes the major deficiencies in existing theoretical/computational approaches and provides unprecedented combination of accuracy and efficiency in modeling light-matter interactions. Once developed, the new computational approach could be applied to many important scientific problems including surface enhanced Raman scattering (SERS), Òborrowed SERSÓ for heterogeneous catalysis, surface-enhanced infrared absorption, surface-enhanced fluorescence, near-field scanning optical microscopy, plasmon-exciton hybridization, plasmon-enhanced photochemistry, photo-induced electron transfer in a single-molecule-junction, and dye-sensitized photovoltaics, etc.

Project Progress

I Introduction

When light interacts with a metallic nanostructure, its conduction electrons may undergo collective oscillations driven by the electric field of the light. Known as localized surface plasmon resonance (LSPR), the collective oscillations can be tuned by adjusting the shape, size and surrounding medium of the nanostructure, which is at the heart of the burgeoning field of plasmonics with potential applications ranging from photocatalysis [1, 2] to optics, chemical and biological sensing [3], and photo-thermal therapeutics, to name but a few [4–8].

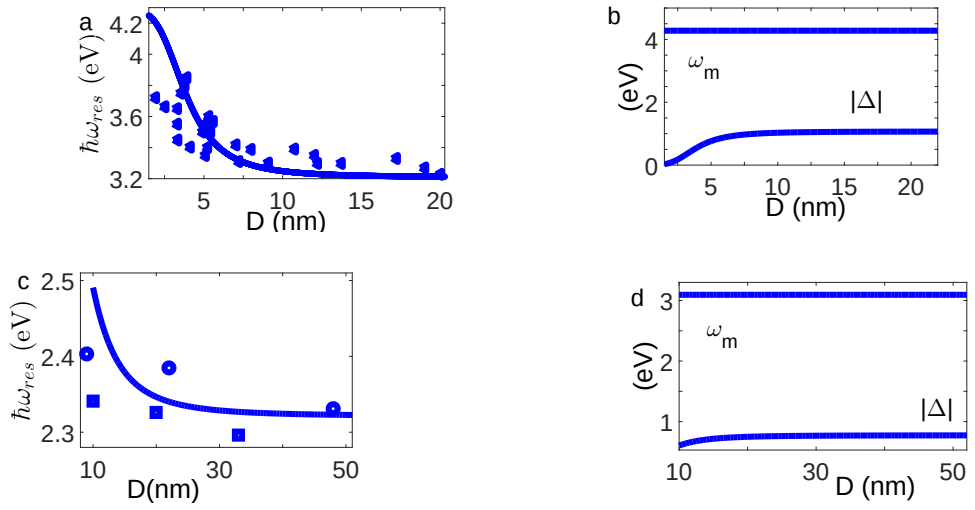

FIG. 1. (a) and (c): The plasmon resonant energy $\hbar\omega_{\rm res}$ as a function of the nano-sphere diameter D, compared between the theory (solid curve) and experimental data (symbols). The triangles in (a) are from the experiment[25] for Ag and the circles and squares in (c) are from reference[30] and reference[31] for Au, respectively. (b) and (d): The contribution of $\omega_{\rm m}$ and $|\Delta|$ as a function of D for Ag and Au, respectively.

Although the fundamental physical theory of light-matter interaction is quantum electrodynamics (QED) [9, 10], traditionally, QED has not been brought to bear on problems in plasmonics. The present research paradigm of plasmonics is rooted in classical electrodynamics where the electromagnetic field of the light is treated classically. It is generally believed that QED correction is too small to be relevant in practical plasmonic applications. The tremendous success of the classical theory has certainly reinforced this notion. However, recently we have found that the QED correction cannot be ignored in plasmonic resonance. In fact, for collective excitations such as LSPR, the QED correction could result in an energy shift on the order of a few tenths of an eV, well within the range of experimental

probes. For nanoparticles, neglecting the correction would lead to a size-dependence of resonant frequency that is contradictory to experiments. In the past few months of the project, we have elucidated the consequence of QED in plasmonics. By focusing on plasmonic resonance of metallic nanostructures, we have illustrated the origin of the plasmonic energy shift and derived analytic expressions for the resonant frequency. The theory is then compared to available experimental results on nano-spheres, nano-rods and nano-plates and shows promise as a rapid means for screening materials and structures in plasmonic applications.

II Theoretical Model

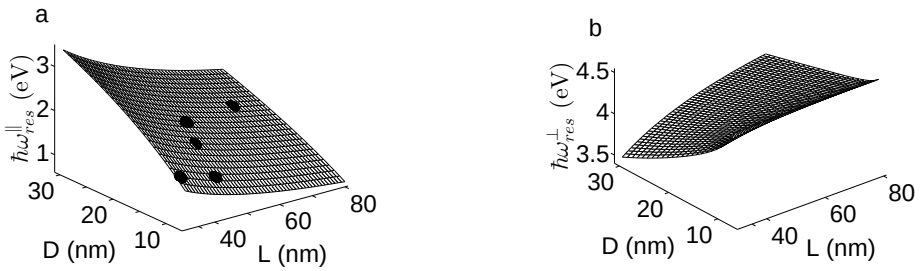

FIG. 2. The plasmonic resonance energy of a Au nano-rod embedded in SiO_2 as a function of its diameter D and length L, compared between the theory (surface) and experiment (dots). The polarization direction is parallel (a) and perpendicular (b) to the nano-rod long-axis.

The present theory of plasmonic resonance rests on a classical description of the electromagnetic field, irrespective of whether the electrons are treated quantum mechanically or not[11–13]. In QED, the electromagnetic field is quantized and there exists a virtual fluctuating electromagnetic field in vacuum carrying zero-point energy. The fluctuating virtual field results in a fluctuation of electronic coordinates, leading to a change in the Coulomb energy between the electrons and the positive ions. This energy change owing to the virtual electromagnetic field is known as Lamb shift in atomic physics, and usually extremely small [10]. In a typical plasmonic nanostructure, the wavelength of the visible light, the beam width and the skin-depth are all greater than the size of the nanostructure [14, 15], hence *all* conduction electrons in the nanostructure undergo coherent and collective oscillations. The higher energy oscillations are longitudinal, corresponding to so-called "bulk" plasmon, while the lower energy oscillations are transverse and correspond to the LSPR. [16] All electrons are involved in both modes of oscillations. For a nanoparticle of a radius of 100 nm, the coherent oscillation could involve $\sim 10^7$ conduction electrons, leading to an induced dipole moment that is 6-7 orders of magnitude stronger than that in an atom. Since the interaction energy of the fluctuating virtual field with the conduction electrons is proportional to the induced dipole, the energy shift can reach several tenths of an eV, which can be measured experimentally.

Let H_e be the electronic Hamiltonian of the nanostructure, and $\{|a\rangle, |b\rangle, \cdots\}$ and $\{E_a, E_b, \cdots\}$ as the eigenstates and eigenvalues of H_e, respectively. Let H_f be the Hamiltonian of the incident electromagnetic field including both the external field and the virtual field. The eigenstates of H_f are labeled as $|n_{\mathbf{k}_1\mathbf{e}_1}, n_{\mathbf{k}_2\mathbf{e}_2} \cdots\rangle$, where $n_{\mathbf{k}_1\mathbf{e}_1}$ is the occupation number in the photon state $\mathbf{k}_1\mathbf{e}_1$ ($\mathbf{k}_1$ is the wave-vector and $\mathbf{e}_1$ is the polarization vector). The total Hamiltonian of the system is thus

$$H = (H_e + H_f) + U, \tag{1}$$

where U is the interaction between the conduction electrons and the virtual field. Since the wavelength of the field is much larger than the size of the nanostructure, the interaction energy U can be expressed as [9, 10]

$$U = -\sum_j \widehat{\mathbf{d}}_j \cdot \mathbf{E}(\mathbf{r}_j), \tag{2}$$

where $\mathbf{E}(\mathbf{r}_j)$ is the electric field at position $\mathbf{r}_j$ of the jth electron, and $\widehat{\mathbf{d}}_j$ is the dipole operator of the jth electron. The extinction spectrum of the nanostructure, comprised of the absorption and scattering spectrum of the incident photon, is the primary physical quantity that can be measured experimentally and calculated theoretically. According to QED [9, 17], the resonant frequency $\omega_{\rm res}$ of the extinction spectrum consists of two contributions:

$$\omega_{\rm res} = \omega_m + \Delta. \tag{3}$$

$\hbar\omega_m$ represents the excitation energy of the plasmons. Since the plasmons or the coherent oscillations are the eigenstates of H_e, denoted by Ψ_m, $\omega_{\rm m}$ is the corresponding eigenfrequency. Δ is the frequency shift resulted from the interaction of the electrons with the virtual field.

Here we derive an analytical expression for this eigenfrequency, with the oscillations along one of the major axes of the nanostructure. To a good approximation, nanostructures such as spheres, rods, and circular plates can be modeled as ellipsoids with a uniform volume polarization. Suppose that a metallic ellipsoid with a dielectric function $\varepsilon_1 = \varepsilon_1' + i\varepsilon_1''$ is embedded in a medium with a dielectric function $\varepsilon_2 = \varepsilon_2' + i\varepsilon_2''$, and the electric field of the incident photon, $E_z^{\rm ext}$, is along the z-axis of the ellipsoid. If the longest dimension the ellipsoid, $L_{\rm max}$, is much smaller than $\lambda\varepsilon_2'^{-1/2}/4$ (λ is the wavelength), the beam width W of the incident light [14], and the skin-depth $\delta = \lambda(2\pi\varepsilon_1''^{1/2})^{-1}$, the quasi-static approximation is valid [15]. The quasi-static approximation implies the phase change across the nanostructure should be small, i.e., $2\pi L_{\rm max}/(\lambda\varepsilon_2'^{-1/2}) \ll \pi/2$. For the violet light with $\lambda = 4000$ Å in vacuum ($\varepsilon_2' = 1$), one arrives at $L_{\rm max} < 100$ nm. In other words, for the nanostructure below 100 nm, the phase retardation is negligible.

Under the quasi-static approximation, the total induced dipole moment in the ellipsoid is given by [15, 16]:

$$\mathcal{P}_{1z} = \alpha_z V \epsilon_0 E_z^{\rm ext}, \text{ with } \alpha_z = \frac{\varepsilon_2(\varepsilon_1 - 1)}{\varepsilon_2 + (\varepsilon_1 - \varepsilon_2)n^{(z)}}. \tag{4}$$

Here V is the volume of the ellipsoid; ϵ_0 is the permeability of free space and $n^{(z)}$ is the depolarization factor along the z-axis. Note that eqn. (4) corresponds to $(\pi L_{\rm max}\varepsilon_2'^{1/2}/\lambda)^3$ terms in the Mie theory [16]. To capture the phase retardation effect in larger nanostructures ($L_{\rm max} > 100$ nm), one can include the higher terms such as $(\pi L_{\rm max}\varepsilon_2'^{1/2}/\lambda)^5$ in the Mie theory, which correspond to the induced electric quadrupole and magnetic dipole of the nanostructure [15].

We now make two assumptions: (1) ε_2' is a constant, which is a reasonable assumption for commonly used media, such as vacuum, SiO_2 and polyvinyl alcohol, in plasmonic applications. (2) The dielectric functions of the nanostructures are primarily determined by the conduction electrons [18], which is also a reasonable approximation. Under these assumptions, the dielectric functions of the nanostructure can be expressed as:

$$\varepsilon_1' = 1 - \frac{S\omega_p^2}{\omega^2 + \gamma^2}, \quad \varepsilon_1'' = \frac{S\gamma\omega_p^2}{\omega^3 + \gamma^2\omega}. \tag{5}$$

Here $\omega_p = (ne^2/m\epsilon_0)^{1/2}$ is the plasmon frequency. n and m denote the electron number density and mass of the electron. $S(\omega)$ represents intra-band oscillator strength of the conduction electrons. γ is the decay rate of the quasiparticles, given by [18–21]:

$$\gamma = \gamma_0 + Av_{\rm F}/L_{\rm eff}, \tag{6}$$

where $v_{\rm F} = \hbar(3\pi^2 n)^{1/3}/m$ is the Fermi velocity of the metal and $L_{\rm eff}$ is the effective dimension of the ellipsoid along the polarization direction. A is a dimensionless, positive constant on the order of one. γ_0 is the decay rate resulting from electron-phonon, electron-impurity, and electron-electron interactions [18], and can be estimated by $\gamma_0 = ne^2/m\sigma$ with σ as the conductivity of the metal. The second term in eqn. (6) stems from electron scattering with the surface, and is the only term dependent on the size of the nanostructure.

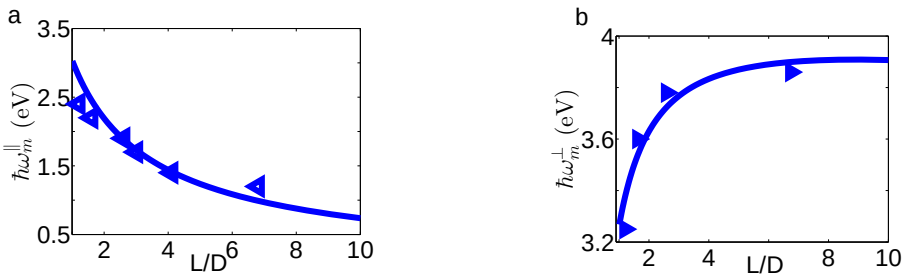

FIG. 3. The eigenfrequency $\omega_{\rm m}$ as a function of L/D for a Na nano-rod in vacuum, determined from the theory (curve) and the TD-OFDFT calculations (triangles). The polarization direction is parallel (a) and perpendicular (b) to the nano-rod long-axis.

Note that the derivation of eqn. (5) is based the free electron model where the wave-functions of the single particle states are Bloch waves. On the other hand, if the shortest dimension of the metallic nanostructure, $L_{\rm min}$, is small,

the corresponding wave-functions are best described standing waves. To ensure that the wave-vectors at the Brillouin zone boundary have an acceptable error ($< 10\%$), $L_{\min}$ has to be greater than 2 nm. Therefore, our analytical results are valid in the size range of 2 nm $< L <$ 100 nm.

In the classical electromagnetism, the extinction cross-section $\sigma_{\rm ex}^{c}(\omega)$ of the nanostructure is[15] proportional to $\{[\varepsilon_2' + (\varepsilon_1' - \varepsilon_2')n^{(z)}]^2 + [\varepsilon_2'' + (\varepsilon_1'' - \varepsilon_2'')n^{(z)}]^2\}^{-1}$. Therefore ω_m is the root of the following equation [22–31]:

$$\varepsilon_2' + (\varepsilon_1' - \varepsilon_2')n^{(z)} = 0. \tag{7}$$

eqn.(7) yields the expression for the eigenfrequency ω_m:

$$\omega_m = \omega_p[\frac{S}{1 + \varepsilon_2'(\frac{1}{n} - 1)} - (\frac{\gamma}{\omega_p})^2]^{1/2}. \tag{8}$$

Here and later we drop the superscript z for brevity when there is no confusion.

Based on non-perturbative many-body quantum theory, the frequency shift Δ can be determined from the Green's function of the Hamiltonian (1). Specifically, $\hbar\Delta$ =Re(R) and R is the shift-operator of the Green's function, given by [9]

$$R = \sum_{a\mathbf{ke}} \frac{|\langle a;\mathbf{ke}|U|\Psi_m;0\rangle|^2}{E_m - E_a - \hbar\omega_{\mathbf{ke}}} + \sum_{a\mathbf{ke}}\sum_{a'\mathbf{k'e'}} \tag{9}$$

$$\frac{\langle\Psi_m;0|U|a;\mathbf{ke}\rangle\langle a;\mathbf{ke}|U|a';\mathbf{k'e'}\rangle\langle a';\mathbf{k'e'}|U|\Psi_m;0\rangle}{(E_m - E_a - \hbar\omega_{\mathbf{ke}})(E_m - E_{a'} - \hbar\omega_{\mathbf{k'e'}})} + \cdots,$$

where E_m is the energy of the eigenstate Ψ_m; $|\Psi_m;0\rangle$ represents the many-body state at which the incident photon is absorbed and the plasmon is excited. $|a;\mathbf{ke}\rangle$ denotes direct-product state of a many-electron state $|a\rangle$ and a virtual photon state with a wave-vector $\mathbf{k}$ and a polarization vector $\mathbf{e}$. Finally, we arrive at

$$\Delta = -\frac{\omega_m}{4}\frac{\beta_z}{1 + \beta_z}, \tag{10}$$

with

$$\beta_z = \frac{V}{\lambda_m^3}\frac{\varepsilon_2'^2}{[n^{(z)}]^2}\{1 + (\frac{\varepsilon_1' - 1}{\varepsilon_1''})^2\}. \tag{11}$$

Here $\lambda_m = 2\pi c/\omega_m$. In eqn. (11), ε_1' and ε_1'' are evaluated at $\omega = \omega_m$. As $\beta_z \geq 0$, the frequency shift Δ is less than 1/4 of ω_m. The central aim of this work is to demonstrate that the interaction of the induced dipole and the vacuum fluctuation of the electromagnetic field causes a red shift Δ of the resonance frequency with increasing the volume of a nanostructure.

According to eqns.(8, 10), there are three contributions to $\omega_{\rm res}$. Among them, the dominant one is the first term in eqn. (8) since $\frac{\gamma}{\omega_p} << 1$; the second term in eqn. (8) is the smallest among them. The dominant term depends *only* on the shape of the nanostructure through the depolarization factor, $n^{(z)}$. Hence the resonant frequency $\omega_{\rm res}$ of the nanostructure is determined primarily by its shape as opposed to its size. This fact has been well established and exploited in plasmonics [22, 23]. More importantly, γ in eqn.(8) is a monotonically decreasing function of $L_{\rm eff}$ as indicated in eqn.(6), hence ω_m is a weakly increasing function of the particle size. If there were no correction term Δ, the resonant frequency $\omega_{\rm res}$ (=ω_m) would have been a monotonically increasing function of the particle size, which is opposite to the experimental observations [21, 24, 25, 30]. The QED correction term, Δ, as a decreasing function of the particle size, reverses the incorrect size-dependence of the classical electromagnetic theory and renders $\omega_{\rm res}$ consistent with the experiments. The failure of the classical theory has also been discussed by Scholl et al. [25] who attributed the opposite size-dependence to the inappropriate use of macroscopic dielectric functions in the nanoparticles. The macroscopic dielectric functions failed to capture the effects of discrete energy levels and the fact that only certain electronic or plasmonic transitions are allowed in the nanoparticles. To remedy the classical theory, Scholl et al. proposed a phenomenological model based on discrete energy levels. Although the model yielded an improved agreement to the experimental data, it did not consider the quantum effect of the electromagnetic field. As a result, the model cannot guarantee the *monotonically* decreasing size-dependence of $\omega_{\rm res}$, as revealed in experiments and the present theory. Nonetheless, Scholl's model is valuable contribution and could be combined with the present theory to form a more comprehensive microscopic picture of plasmonic resonance.

If the electric field of the incident light is perpendicular to the z-axis, the depolarization factor in the normal direction has to be worked out. We have derived the corresponding equations. Moreover, if the electric field of the incident light is along an arbitrary direction, the total induced dipole is a vector sum of the components in each major axis [15, 16]. Finally, for a spheroid with its rotational axis along z, the depolarization factors $n^{(x)}$, $n^{(y)}$, $n^{(z)}$ and the resonant frequency $\omega_{\rm res}^{\parallel}$ ($\mathbf{E}_{\rm ext}$ $\|$z) and $\omega_{\rm res}^{\perp}$ ($\mathbf{E}_{\rm ext}$ $\perp$z) can be calculated analytically as well. For a general ellipsoid, the corresponding quantities have to be evaluated numerically.

The size dependence of plasmonic resonance frequency in metallic nanostructures has been studied extensively and several physical origins have been proposed, including size-dependent dielectric functions [25, 32, 33], phase retardation [34, 35], and nonlocal response of current to the electromagnetic field [36–43], etc. However, in all previous works, the electromagnetic field was treated classically.

III Results and Discussion

To validate the proposed theory, we apply it to various metallic nanostructures including nano-spheres, nano-rods, and nano-plates. First, we examine the size-dependence of $\omega_{\rm res}$ in nano-spheres. Since all spheres have the same shape or the depolarization factors [15] ($n = 1/3$), the nano-spheres of the same metal would yield the same ω_m for a given surrounding medium. According to eqns.(10, 11), Δ depends only on the volume of a sphere, thus $\omega_{\rm res}$ is a monotonically decreasing function of the sphere diameter D. When comparing to experimental results for nanoparticles, one should be cautious. This is because in most experiments where plasmon resonance of nanoparticles is measured, the nanoparticles are often covered by ligands. Since the ligands tend to attract electrons from the nanoparticles, the measured resonant energies may deviate considerably from their intrinsic values, for which the theoretical model is developed. More importantly, nanoparticles with different sizes are affected differently by the ligands (the smaller the particle, the greater the effect), thus yielding different size-dependence of the resonance energy. To avoid this problem, we choose to focus on experiments where the nanoparticles are ligand-free. One such experiment which has attracted a lot attention is the work of Scholl et al. [25] who have measured the plasmon resonance of individual ligand-free Ag nanoparticles using aberration-corrected transmission electron microscope (TEM) and monochromated scanning TEM electron energy-loss spectroscopy. In Fig. 1(a), we compare the theoretical prediction to the experimental data taken from Fig. 3(b) of Scholl's paper [25]. The dielectric constant of the surrounding medium ε_2' is 1.69 as measured in the experiment. We find that the theoretical prediction agrees very well to the experimental data as long as the two fitting parameters A and S are chosen reasonably, in this case $A = 0.03,\ S = 1$. It is important to point out that the present theory predicts the correct experimental trend - a *monotonic* redshift as D increases, regardless the choice of A and S. As displayed in Fig. 1(b), the size dependence of $\omega_{\rm res}$ is entirely contained in Δ while ω_m is essentially flat. Thus the size-dependence of the nano-spheres originates exclusively from the quantum nature of the electromagnetic field. To the best of our knowledge, the present theory is the only one that yields the correct experimental trend for ligand-free nanoparticles in the range between 2 nm and 20 nm. For example, quantum mechanical calculations based on self-consistent hydrodynamic model predicted a redshift first then a blueshift as the particle diameter increases [44]. The quantum mechanical time-dependent orbital-free density functional theory (TD-OFDFT) calculations reported a redshift first, then a blueshift and then a redshift again as the particle diameter varies from 1 nm to 12 nm [45]. The time-dependent DFT calculations reported a blueshift for small particles less than 2 nm [46]. It is important to point out, however, that the electric quadrupole, magnetic dipole and phase retardation can also lead to the redshift, but for much larger particles ($>$ 100 nm). [16] Similar comparison is made for gold nano-spheres embedded in water whose dielectric constant $\varepsilon_2' = 1.78$. As shown in Fig. 1(c) and 1(d), the fitting parameters are $A = 0.01$, $S = 0.54$.

Second, we compare the theoretical prediction to the experimental results for Au nano-rods embedded in silica [23] ($\varepsilon_2' = 2.15$). In Fig. 2 (a), the experimental resonance frequency $\omega_{\rm res}^{\parallel}$ as function of the length L and diameter D of the nano-rods is shown in circles, while the theoretical prediction is on the surface. In this case, the two fitting parameters are $A = 0.6,\ S = 1.4$. Because L is $\sim$ 32-70 nm [23], larger than the size of the nano-spheres, the electron scattering at the surface becomes more important, thus A is larger. For the similar reason, the oscillator strength S is also larger than the nano-spheres. There is an overall good agreement between the theory and experiment, down to the size of 8.5 nm [23]. The theoretical prediction for the polarization direction perpendicular to the nano-rod axis is displayed in Fig. 2 (b).

We next demonstrate the validity of ω_m, which cannot be measured directly by experiments. Hence, we compare the theoretical prediction of ω_m to a set of computational results obtained from TD-OFDFT simulations [45, 47] for a Na nano-rod embedded in vacuum (ε_2'=1). A number of (L, D) combinations including (5.79,0.86), (5.79,1.41), (5.79,1.93), (5.79,2.23), (5.79,3.54), (5.79,4.76), and (5.79,5.46), in the unit of nm, are considered. The two fitting parameters are $A = 0.6,\ S = 0.8$ for $\mathbf{E} \parallel$ axis and $A = 0.6,\ S = 0.92$ for $\mathbf{E} \perp$ axis. There is an excellent agreement between the theoretical predictions and the TD-OFDFT results for both polarization directions as shown in Fig. 3,

which validates the derivation of ω_m. In Fig. 2 and 3, one may notice that $\hbar\omega^{\parallel}_{\rm res}(L,D)$ has an opposite size-dependence as $\hbar\omega^{\perp}_{\rm res}(L,D)$, owing to the opposite (L,D) dependence of $n^{(z)}$ and $n^{(x)}$.

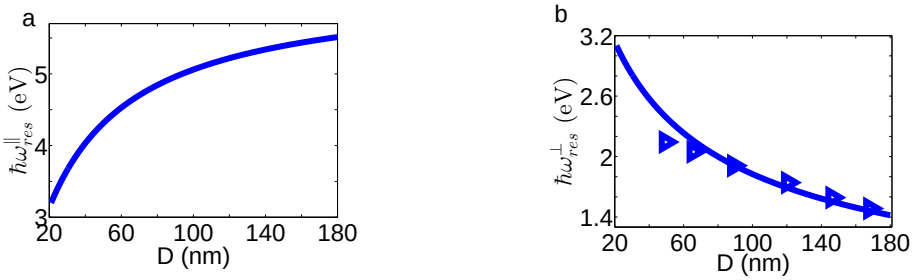

FIG. 4. The plasmonic resonance energy as a function of diameter D for a circular gold nano-plate with a fixed height $L =$ 20 nm. The results from theory are shown in solid curves while the experimental data is shown as triangles; The polarization direction is parallel (a) and perpendicular (b) to the long-axis of the plate.

Third, we switch to a Au nano-plate whose rotational symmetric axis is along z. The theoretical predictions for $\omega^{\perp}_{\rm res}(D)$ are compared to the experimental results [22]. The circular nano-plate has a height $L = 20$nm embedded in a medium with a refractive index of 1.26. The fitting parameters $A = 0.6$, $S = 0.86$ yield an excellent agreement between the theoretical predictions and the experimental data as shown in Fig. 4. Similar agreement between the theory and experiments is also observed for Al and Pt nano-plates which is presented in the Supplementary Information. The opposite D-dependence between $\omega^{\parallel}_{\rm res}(D)$ and $\omega^{\perp}_{\rm res}(D)$ is due to the opposite D-dependence of their respective depolarization factors.

Although size-dependent dielectric functions could be invoked to explain the size-dependence of $\omega_{\rm res}$, such explanation is restricted to small nanoparticles. One can estimate the maximum radius R of the nanoparticles above which the size-dependent dielectric functions become indistinguishable from the bulk dielectric functions. It is known that the presence of discrete energy levels is the origin of the size-dependent dielectric functions [25]. Hence if the level spacing becomes comparable or smaller than $\hbar\gamma_0$ ($\gamma_0 = v_F/l$ where l is the mean free path of bulk material), the dielectric functions are no longer size-dependent. This condition leads to $R \sim \pi(\hbar l/8mv_F)^{1/2}$. Taking $l \sim 10^3$ Å, $v_F \sim 3\times10^6$ m/s, we have $R \sim 2.2$ nm. Clearly, for the size range $2 < L_{\rm max} < 100$ nm discussed in this work, the size-dependence of $\omega_{\rm res}$ cannot be described by the size-dependent dielectric functions. The QED formalism provides a plausible framework whose predictions agree well with the experimental observations.

QED could have more profound implications in plasmonics than what is presented in this report. For example, it is known that when a nano-antenna is placed next to a metallic nanostructure, there is an interaction between the nano-antenna (an emitter) and the virtual field. The interaction could change the directional radiation pattern of the antenna [48], analogous to cavity QED [49]. The present work, on the other hand, focuses on the interaction between an absorber (the plasmonic nanostructure) and the virtual field. Such interaction could also change the induced magnetic moment of the metallic nanostructure, as well as the polarization of the incident light.

IV Summary

To summarize, we propose that QED is important to understand the plasmonic resonance in metallic nanostructures, specially nanoparticles. The coherent motion of the conduction electrons in the nanostructure could lead to a large induced dipole moment, which interacts with the virtual field and results in a significant shift in the resonant frequency. The frequency shift is the key to reconciling the theoretical predictions and experimental observations on size-dependent plasmonic resonance. Based on QED, we have derived analytic expressions for the plasmonic resonant frequency, which depends on three easily accessible material parameters - the dielectric constant ε_2' of the surrounding medium, the number density n of electrons and the conductivity σ of the metal. The analytic expression are shown to reproduce very well the experimental data for nano-spheres, nano-rods and nano-plates, and can be used readily for estimating the resonant frequency of plasmonic nanostructures as a function of their geometry, composition and surrounding medium.

[1] Mukherjee, S., Libisch, F., Large, N., Neumann, O., Brown, L. V., Cheng, J., Lassiter, J. B., Carter, E. A., Nordlander, P., and Halas, N. J. Hot Electrons Do the Impossible: Plasmon-Induced Dissociation of H_2 on Au, Nano Lett.**13**, 240-247,

(2013).
[2] Linic, S., Aslam, U., Boerigter, C., Morabito, M. Photochemical transformations on plasmonic metal nanoparticles. Nature Materials **14** 567-576 (2015).
[3] Mayer, K. M., Hafner, J. H. Localized Surface Plasmon Resonance Sensors. Chemical Reviews, **111**, 3828-3857 (2011).
[4] Halperin, W.P. Quantum size effects in metal particles. Rev. Mod. Phys. **58**, 533-606 (1986).
[5] Link, S., El-Sayed, M. A. Optical properties and ultrafast dynamics of metallic nanocrystals. Annu. Rev. Phys. Chem. **54**, 331-366 (2003).
[6] Kalsin, A., Fialkowski, M., Paszewski, M., Smoukov, S. K., Bishop, K. J. M., Grzybowski, B. A. Electrostatic Self-Assembly of Binary Nanoparticle Crystals with a Diamond-Like Lattice. Science **312**, 420-424 (2006).
[7] Stuart, D. A.; Yuen, J. M., Shah, N.; Lyandres, O., Yonzon, C. R., Glucksberg, M. R., Walsh, J. T., Duyne, P. V. In Vivo Glucose Measurement by Surface-Enhanced Raman Spectroscopy. Anal. Chem. **78**, 7211-7215 (2006).
[8] Huang, X., El-Sayed, I. H., Qian, W., El-Sayed, M. A. Cancer Cell Imaging and Photothermal Therapy in the Near-Infrared Region by Using Gold Nanorods. J. Am. Chem. Soc. **128**, 2115-2120 (2006).
[9] Cohen-Tannoudji, C., Dupont-Roc, J., Grynberg, G. *Atom - Photon Interactions*: Basic Process and Applications, John Wiley, New York (1992).
[10] Berestetskii, V. B., Lifshitz, E. M., Pitaevskiĭ, L. P. *Quantum Electrodynamics*, Butterworth-Heinemann (1982).
[11] Kulkarni, V., Prodan, E., Nordlander, P., Quantum Plasmonics: Optical Properties of a Nanomatryushka, Nano Lett. **13**, 5873 (2013).
[12] Song, P., Meng S., Nordlander, P., Gao, S., Quantum plasmonics: Symmetry-dependent plasmon-molecule coupling and quantized photoconductances, Phys. Rev. B **86**, 121410 (2012).
[13] Morton, S. M., Silverstein, D. W., Jensen, L., Theoretical Studies of Plasmonics using Electronic Structure Theory, Chem. Rev., **111**, 3962-3994, (2011).
[14] Crawford, F. S. *Waves*, McGraw-Hill, New York (1968).
[15] Landau, L. D., Lifshitz E. M. and Pitaevskii, L. P. *Electrodynamics of Continuous Media*, Second Edition, Butterworth, Amsterdam (1984).
[16] Stratton, J. A. *Electromagnetic Theory*, McGraw-Hill, New York (1941).
[17] Bruun, G. M., Jackson, A. D., Kolomeitsev, E. E., Multichannel scattering and Feshbach resonances: Effective theory, phenomenology, and many-body effects, Phys. Rev. A **71**, 052713 (2005).
[18] Callaway, J. *Quantum Theory of the Solid State*, 2nd ed., Academic Press, Boston (1991).
[19] Lee K.-S. and El-Sayed, M. A. Dependence of the Enhanced Optical Scattering Efficiency Relative to That of Absorption for Gold Metal Nanorods on Aspect Ratio, Size, End-Cap Shape, and Medium Refractive Index. J. Phys. Chem B. **109**, 20331-20338 (2005).
[20] Coronado, E.A., and Schatz, G. C., Surface plasmon broadening for arbitrary shape nanoparticles: A geometrical probability approach. J. Chem. Phys. **119**, 3926-3934 (2003).
[21] Jain, P. K., Lee, K. S., El-Sayed, I. H., El-Sayed, M. A. Calculated Absorption and Scattering Properties of Gold Nanoparticles of Different Size, Shape, and Composition: Applications in Biological Imaging and Biomedicine. J. Phys. Chem B. **110**, 7238-7248 (2006).
[22] Zorić, I., Zäch, M., Kasemo, B. and Langhammer, C. Gold, Platinum, and Aluminum Nanodisk Plasmons: Material Independence, Subradiance, and Damping Mechanisms. ACS Nano **3**, 2535-2546 (2011).
[23] Juvé, V., Cardinal, M. F., Lombardi, A., Crut, A., Maioli, P., Perez-Juste, J., Liz-Marzan, L. M., Fatti, N. D. and Vallee, F. Size-Dependent Surface Plasmon Resonance Broadening in Nonspherical Nanoparticles: Single Gold Nanorods. Nano Lett. **13**, 2234-2240 (2013).
[24] Baida, H.,Billaud, P., Marhaba, S., Christofilos, D., Cottancin, E., Crut, A., Lermé, J., Maioli, P., Pellarin, M., Broyer, M., Del Fatti, N., Vallée, F., Sánchez-Iglesias, A., Pastoriza-Santos I. and Liz-Marzán, L. M. Quantitative Determination of the Size Dependence of Surface Plasmon Resonance Damping in Single Ag@SiO_2 Nanoparticles. Nano Lett. **9**, 3463-3469 (2009).
[25] Scholl, J. A., Koh A. L. and Dionne, J. A. Quantum plasmon resonances of individual metallic nanoparticles. Nature **483**, 421-427 (2012).
[26] Klar, T., Perner, M., Grosse, S. von Plessen, G., Spirkl, W., and Feldmann, J., Surface-Plasmon Resonances in Single Metallic Nanoparticles. Phys. Rev. Lett. **80**, 4249-4252 (1998).
[27] Voisin, C., Fatti, N, D., Christofilos, D., and Vallée, F. Ultrafast Electron Dynamics and Optical Nonlinearities in Metal Nanoparticles. J. Phys. Chem. B **105**, 2264-2280 (2001).
[28] Kreibig, U. Small Silver Particles in Photosensitive Glass. Appl. Phys.**10**, 255-264 (1976).
[29] C. Noguez, J. Phys. Chem. C **111**, 3806-3819 (2007).
[30] Link S., and El-Sayed, M. A. Size and Temperature Dependence of the Plasmon Absorption of Colloidal Gold Nanoparticles. J. Phys. Chem B **103**, 4212-4217 (1999).
[31] Berciaud, S., Cognet, L., Tamarat, P., and Lounis, B. Observation of Intrinsic Size Effects in the Optical Response of Individual Gold Nanoparticles. Nano Lett. **5**, 515-518 (2005).
[32] E. Ringe, J. Zhang, M. R. Langille, K. Sohn, C. Cobley, L. Au, Y. Xia, C. A. Mirkin, J. Huang, L. D. Marks & R. P. Van Duyne, Mater. Res. Soc. Symp. Proc. **1208**, 1208-O10-02, (2010).
[33] M. Losurdo, M. M. Giangreorio, G. V. Bianco, A. A. Suvorova, C. Kong, S. Rubanov, P. Capezzuto, J. Humlicek, and G. Bruno, Phys. Rev. B **82**, 155451 (2010).
[34] T. J. Davis, K. C. Vernon, and D. E. Gómez, Optics Express **17**, 23655-23663 (2009).
[35] O. Lecarme, Q. Sun, K. Ueno, & H. Missawa, ACS Photonics **1**, 538 (2014).

[36] R. J. Pollard, A. Murphy, W. R. Hendren, P. R. Evans, R. Atkinson, G. A. Wurtz, A. V. Zayats, and Viktor A. Podolskiy, Phys. Rev. Lett. **102**, 127405 (2009).
[37] B. M. Wells, A. V. Zayats and V. A. Podolskiy, Quantum Electronics and Laser Science Conference 2012, San Jose, California United States 6–11 May 2012.
[38] Alexey A. Orlov, Pavel M. Voroshilov, Pavel A. Belov, and Yuri S. Kivshar, Phys. Rev.B **84**, 045424 (2011).
[39] G. Toscano, M. Wubs, S. Xiao, M.Yan, Z. F. Ozturk, A.-P. Jauho and N. Asger Mortensen, Plasmonics: Metallic Nanostructures and Their Optical Properties VIII, edited by Mark I. Stockman, Proc. of SPIE **7757**, doi: 10.1117/12.860774 (2010).
[40] G. Miano1, G. Rubinacci, A. Tamburrino, and F. Villone, IEEE Transactions on Magnetics **44**, 822 (2008).
[41] R. Chang, H.-P. Chiang, P.T. Leung, W. S. Tse, Optics Communications **225**, 353 (2003).
[42] F. J. G. de Abajo, J. Phys. Chem. C **112**, 17983 (2008).
[43] A. Moradi, Physics of Plasmas 22, 032112 (2015).
[44] G. Toscano, J. Straubel, A. Kwiatkowski, C Rockstuhl, F. Evers, H. Xu, N. A. Mortensen & M. Wubs, Resoance shift and spill-out effects in self-consistent hydrodynamic nanoplasmonics, Nature Comm. DOI: 10.1038/ncomms8132 (2015).
[45] Xiang, H. P., Zhang, X., Neuhauser, D. and Lu, G. Size-Dependent Plasmonic Resonances from Large-Scale Quantum Simulations. J. Phys. Chem. Lett. **5**, 1163-1169 (2014).
[46] M. Kuisma, A. Sakko, T. P. Rossi, A. H. Larsen, J. Enkovaara, L. Lehtovaara, and T. T. Rantala, Phys. Rev. B **91**, 115431 (2015).
[47] D.Neuhauser, S. Pistinner, A. Coomar, X. Zhang and G. Lu, Dynamic kinetic energy potential for orbital-free density functional theory, J. Chem.Phys. **134**, 144101 (2011).
[48] Giannini, V., Fernandez-Domínguez, A. I., Heck, S. C. and Maier, S. A. Plasmonic nanoantennas: fundamentals and their use in controlling the radiative properties of nanoemitters. Chem. Rev. **111**, 3888 (2011).
[49] Haroche, S. Controlling photons in a box and exploring the quantum to classical bounday. Rev. Mod. Phys. **85**, 1083-1102 (2013).